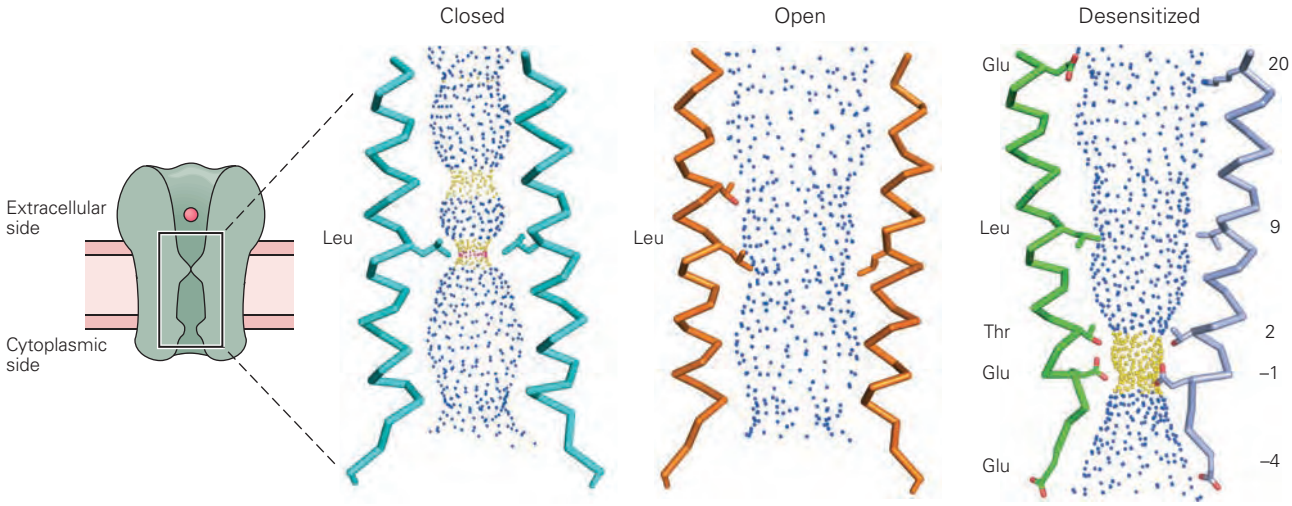

Figure 12–12 A high-resolution three-dimensional structural model of a neuronal nicotinic ACh receptor-channel. High-resolution models of the pentameric family of ligand-gated channels are shown for the closed, open, and desensitized states of the receptor-channel. Two out of five of the M2 α-helixes are shown. The desensitized structure is from the human neuronal ACh receptor. The closed and open states are based on structures of neuronal glycine receptors, which are closely related in amino acid sequence to ACh receptor subunits. Key amino acid side chains are illustrated for the desensitized ACh receptor with position numbering on the right and amino acid abbreviations on the left. According to convention, position 0 is near the intracellular surface of the phospholipid bilayer; other positions are labeled according to relative position in the primary amino acid sequence. A conserved leucine in the middle of the M2 segment (position 9) forms a gate that constricts the pore in the closed state. Ligand binding causes the subunits to tilt outward and twist, opening up the leucine gate. A further conformational change during desensitization causes the subunits to tilt inward near the bottom, constricting the pore near the intracellular side of the channel and thereby producing a nonconducting state. The negatively charged glutamates at positions 20, –1, and –4 correspond to the external (**1**), middle (**2**), and internal (**3**) rings of charge in Figure 12–11C. The negatively charged glutamate at position –1 and the electronegative threonine at position 2 form the selectivity filter of the channel. (Reproduced, with permission, from Morales-Perez et al. 2016. Copyright © 2016 Springer Nature.)

M3 transmembrane segments. This motion exerts a force on the M2 segment that leads to its rotation and tilting, thereby opening up the hydrophobic leucine gate in the middle of the pore and allowing ion permeation. Although future studies will no doubt refine our understanding of the structural bases for nicotinic receptor-channel and function, these recent advances give us an unprecedented molecular understanding of one of the most fundamental processes in the nervous system: synaptic transmission and, specifically, the signaling of information from nerve to muscle.

Highlights

1. The terminals of motor neurons form synapses with muscle fibers at specialized regions in the muscle membrane called end-plates. When an action potential reaches the terminals of a presynaptic motor neuron, it causes the release of ACh.
2. ACh diffuses across the narrow (100-nm) synaptic cleft in a matter of microseconds and binds to nicotinic ACh receptors in the end-plate membrane. The energy of binding is translated into a conformational change that opens a cation-selective channel in the protein, allowing Na^+, K^+, and Ca^{2+} to flow across the postsynaptic membrane. The net effect, due largely to the influx of Na^+ ions, produces a depolarizing synaptic potential called the end-plate potential.
3. Because the ACh receptor-channels are concentrated at the end-plate, the opening of these channels produces a local depolarization. This local depolarization is large enough (75 mV) to exceed the threshold for action potential generation by a factor of three to four.
4. It is important that the safety factor of nerve-muscle transmission be at a high level, as it determines our ability to move, breath, and escape from danger. Decreases in ACh receptor number or function as a result of autoimmune disease or genetic mutations can contribute to neurological disorders.
5. Patch-clamp recordings have revealed the step-like increase and decrease in current in response to the opening and closing of single ACh receptor-channels. A typical excitatory postsynaptic current

at the neuromuscular junction is generated by the opening of approximately 200,000 individual channels.

6. The biochemical structure of the muscle nicotinic ACh receptor has been determined. The receptor is a pentamer composed of two α-subunits and one β-γ-, and δ-subunit. The four genes encoding the subunits are closely related, and more distantly related to the genes encoding other pentameric ligand-gated channels for other transmitters.
7. Higher-resolution structures have provided a detailed view of the ACh ligand-binding pocket and the pore of the channel and further insight into how ligand binding leads to conformational changes associated with receptor-channel opening and desensitization gating reactions.

Postscript: The End-Plate Current Can Be Calculated From an Equivalent Circuit

The current through a population of ACh receptor-channels can be described by Ohm's law. However, to describe how the current generates the end-plate potential, the conductance of the resting channels in the surrounding membrane must also be considered. We must also take into consideration the capacitive properties of the membrane and the ionic batteries determined by the distribution of Na^+ and K^+ inside and outside the cell.

The dynamic relationships between these various components can be explained using the same rules we used in Chapter 9 to analyze the current in passive electrical devices that consist only of resistors, capacitors, and batteries. We can represent the end-plate region with an equivalent circuit that has three parallel current paths: (1) one for the synaptic current through the transmitter-gated channels, (2) one for the return current through resting channels (the nonsynaptic membrane), and (3) one for the capacitive current across the lipid bilayer (Figure 12–13). For simplicity, we ignore the voltage-gated channels in the surrounding nonsynaptic membrane.

Because the end-plate current is carried by both Na^+ and K^+ flowing through the same ion channel, we combine the Na^+ and K^+ current pathways into a single conductance (g_{EPSP}) representing the ACh receptor-channels. The conductance of this pathway is proportional to the number of channels opened, which in turn depends on the concentration of transmitter in the synaptic cleft. In the absence of transmitter, no channels are open and the conductance is zero. When a presynaptic action potential causes the release

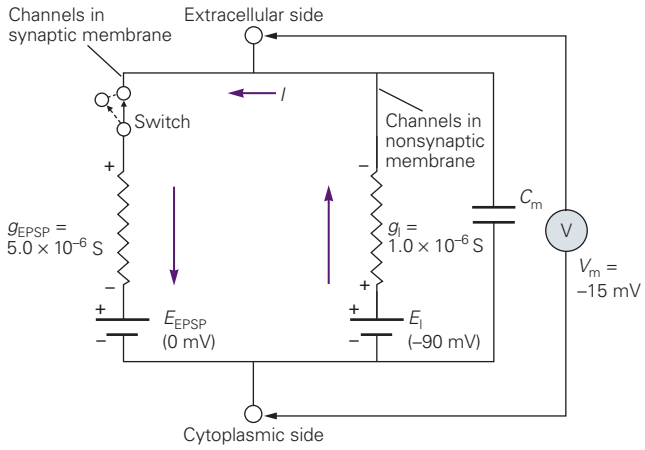

Figure 12–13 The equivalent circuit of the end-plate. The circuit has three parallel current pathways. One conductance pathway carries the end-plate current and consists of a battery (E_{EPSP}) in series with the conductance of the ACh receptor-channels (g_{EPSP}). Another conductance pathway carries current through the nonsynaptic membrane and consists of a battery representing the resting potential (E_l) in series with the conductance of the resting channels (g_l). In parallel with both of these conductance pathways is the membrane capacitance (C_m). The voltmeter (V) measures the potential difference between the inside and the outside of the cell.

When no ACh is present, the ACh receptor-channels are closed and carry no current. This state is depicted as an open electrical circuit in which the synaptic conductance is not connected to the rest of the circuit. The binding of ACh opens the synaptic channels. This event is electrically equivalent to throwing the switch that connects the gated conductance pathway (g_{EPSP}) with the resting pathway (g_l). In the steady state, an inward current through the ACh receptor-channels is balanced by an outward current through the resting channels. With the indicated values of conductances and batteries, the membrane will depolarize from –90 mV (its resting potential) to –15 mV (the peak of the end-plate potential).

of ACh, the conductance of this pathway increases to approximately 5×10^{-6} S, which is about five times the conductance of the parallel branch representing the resting (leakage) channels (g_l).

The end-plate conductance is in series with a battery (E_{EPSP}) with a value given by the reversal potential for synaptic current (0 mV) (Figure 12–13). This value is the weighted algebraic sum of the Na^+ and K^+ equilibrium potentials (see Box 12–1). The current during the excitatory postsynaptic potential (I_{EPSP}) is given by

$$I_{EPSP} = g_{EPSP} \times (V_m - E_{EPSP}).$$

Using this equation and the equivalent circuit of Figure 12–13, we can now analyze the EPSP in terms of its components (Figure 12–14).

At the onset of the EPSP (the dynamic phase), an inward current (I_{EPSP}) flows through the ACh

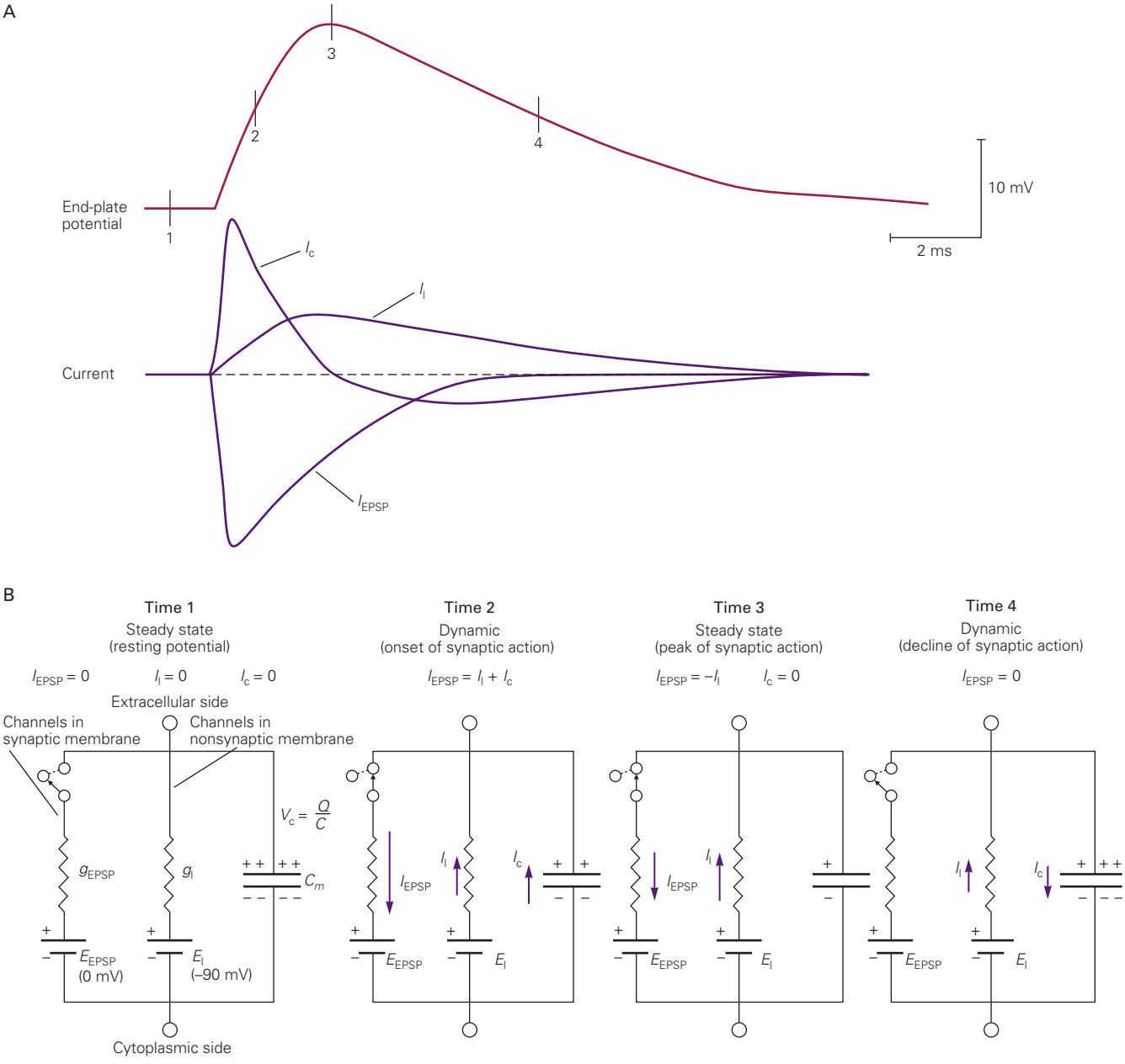

Figure 12–14 The time course of the end-plate potential is determined by both the ACh-gated synaptic conductance and the passive membrane properties of the muscle cell.

A. The time course of the end-plate potential and the component currents through the ACh receptor-channels (I_{EPSP}), the resting (or leakage) channels (I_l), and the capacitor (I_c). There is a capacitive current only when the membrane potential is changing. In the steady state, such as at the peak of the end-plate potential, the inward flow of positive charge through the ACh receptor-channels is exactly balanced by the outward ionic current across the resting channels, and there is no capacitive current.

B. Equivalent circuits for the current at times 1, 2, 3, and 4 shown in part A. (The relative magnitude of a current is represented by the arrow length.)

receptor-channels because of the increased conductance to Na^+ and K^+ and the large inward driving force on Na^+ at the resting potential of –90 mV (Figure 12–14B, time 2). Because charge flows in a closed loop, the inward synaptic current leaves the cell as outward current through two parallel pathways: a pathway for ionic current (I_l) through the resting (or leakage) channels and a pathway for capacitive current (I_c) across the lipid bilayer. Thus,

$$I_{EPSP} = -(I_l + I_c).$$

During the earliest phase of the EPSP, the membrane potential, V_m, is still close to its resting value, E_l. As a result, the outward driving force on current through the resting channels ($V_m - E_l$) is small. Therefore, most of the outward current leaves the cell as capacitive current and the membrane depolarizes rapidly (Figure 12–14B, time 2). As the cell depolarizes, the outward driving force on current through the resting channels increases, while the inward driving force on synaptic current through the ACh receptor-channels decreases. Concomitantly, as the concentration of ACh in the synapse decreases, the ACh receptor-channels begin to close, and eventually the inward current through the gated channels is exactly balanced by outward current through the resting channels ($I_{EPSP} = -I_l$). At this point, no charge flows into or out of the capacitor ($I_c = 0$). Because the rate of change of membrane potential is directly proportional to I_c,

$$I_c / C_m = \Delta V_m / \Delta t,$$

the membrane potential will have reached a peak or new steady-state value, $\Delta V_m / \Delta t = 0$ (Figure 12–14B, time 3).

As the ACh receptor-channels close, I_{EPSP} decreases further. Now I_{EPSP} and I_l are no longer in balance and the membrane potential starts to repolarize, because the outward current through leak channels (I_l) becomes larger than the inward synaptic current. During most of the declining phase of the synaptic action, the ACh receptor-channels carry no current because they are all closed. Instead, current is conducted through the membrane only as outward current carried by resting channels, balanced by inward capacitive current (Figure 12–14B, time 4).

When the EPSP is at its peak or steady-state value, $I_c = 0$, and therefore the value of V_m can be easily calculated. The inward current through the ACh receptor-channels (I_{EPSP}) must be exactly balanced by outward current through the resting channels (I_l):

$$I_{EPSP} + I_l = 0. \qquad \textbf{(12–7)}$$

The current through the ACh receptor-channels (I_{EPSP}) and resting channels (I_l) is given by Ohm's law:

$$I_{EPSP} = g_{EPSP} \times (V_m - E_{EPSP}),$$

and

$$I_l = g_l \times (V_m - E_l).$$

By substituting these two expressions into Equation 12–7, we obtain

$$g_{EPSP} \times (V_m - E_{EPSP}) + g_l \times (V_m - E_l) = 0.$$

Solving for V_m, we obtain

$$V_m = \frac{(g_{EPSP} \times E_{EPSP}) + (g_l \times E_l)}{g_{EPSP} + g_l}. \qquad \textbf{(12–8)}$$

This equation is similar to that used to calculate the resting and action potentials (Chapter 9). According to Equation 12–8, the peak voltage of the EPSP is a weighted average of the electromotive forces of the two batteries for the ACh receptor-channels and the resting (leakage) channels. The weighting factors are given by the relative magnitude of the two conductances. Since g_l is a constant, the greater the value of g_{EPSP} (ie, the more ACh channels are open), the more closely V_m will approach the value of E_{EPSP}.

We can now calculate the peak EPSP for the specific case shown in Figure 12–13, where $g_{EPSP} = 5 \times 10^{-6}$ S, $g_l = 1 \times 10^{-6}$ S, $E_{EPSP} = 0$ mV, and $E_l = -90$ mV. Substituting these values into Equation 12–8 yields

$$V_m = \frac{[(5 \times 10^{-6}\ \text{S}) \times (0\ \text{mV})] + [(1 \times 10^{-6}\ \text{S}) \times (-90\ \text{mV})]}{(5 \times 10^{-6}\ \text{S}) + (1 \times 10^{-6}\ \text{S})}.$$

or

$$V_m = \frac{(1 \times 10^{-6}\ \text{S}) \times (-90\ \text{mV})}{(6 \times 10^{-6}\ \text{S})} = -15\ \text{mV}.$$

The peak amplitude of the EPSP is then

$$\Delta V_{EPSP} = V_m - E_l = -15\ \text{mV} - (-90\ \text{mV}) = 75\ \text{mV}.$$

Gerald D. Fischbach
Steven A. Siegelbaum

Selected Reading

Fatt P, Katz B. 1951. An analysis of the end-plate potential recorded with an intracellular electrode. J Physiol 115:320–370.

Heuser JE, Reese TS. 1977. Structure of the synapse. In: ER Kandel (ed). *Handbook of Physiology: A Critical, Comprehensive Presentation of Physiological Knowledge and Concepts*, Sect. 1 *The Nervous System*, Vol. 1 *Cellular Biology of Neurons*, Part 1, pp. 261–294. Bethesda, MD: American Physiological Society.

Hille B. 2001. *Ion Channels of Excitable Membranes*, 3rd ed., pp. 169–199. Sunderland, MA: Sinauer.

Imoto K, Busch C, Sakmann B, et al. 1988. Rings of negatively charged amino acids determine the acetylcholine receptor-channel conductance. Nature 335:645–648.

Karlin A. 2002. Emerging structure of the nicotinic acetylcholine receptors. Nat Rev Neurosci 3:102–114.

Neher E, Sakmann B. 1976. Single-channel currents recorded from membrane of denervated frog muscle fibres. Nature 260:799–802.

Nemecz Á, Prevost MS, Menny A, Corringer PJ. 2016. Emerging molecular mechanisms of signal transduction in pentameric ligand-gated ion channels. Neuron 90:452–470.

References

Akabas MH, Kaufmann C, Archdeacon P, Karlin A. 1994. Identification of acetylcholine receptor-channel lining residues in the entire M2 segment of the α-subunit. Neuron 13:919–927.

Alberts B, Bray D, Lewis J, Raff M, Roberts K, Watson JD. 1989. *Molecular Biology of the Cell*, 2nd ed. New York: Garland.

Brejc K, van Dijk WJ, Klaassen RV, et al. 2001. Crystal structure of an ACh-binding protein reveals the ligand-binding domain of nicotinic receptors. Nature 411:269–276.

Charnet P, Labarca C, Leonard RJ, et al. 1990. An open channel blocker interacts with adjacent turns of α-helices in the nicotinic acetylcholine receptor. Neuron 4:87–95.

Claudio T, Ballivet M, Patrick J, Heinemann S. 1983. Nucleotide and deduced amino acid sequences of *Torpedo californica* acetylcholine receptor γ-subunit. Proc Natl Acad Sci U S A 80:1111–1115.

Colquhoun D. 1981. How fast do drugs work? Trends Pharmacol Sci 2:212–217.

Dwyer TM, Adams DJ, Hille B. 1980. The permeability of the endplate channel to organic cations in frog muscle. J Gen Physiol 75:469–492.

Fertuck HC, Salpeter MM. 1974. Localization of acetylcholine receptor by ^{125}I-labeled α-bungarotoxin binding at mouse motor endplates. Proc Natl Acad Sci U S A 71:1376–1378.

Heuser JE, Salpeter SR. 1979. Organization of acetylcholine receptors in quick-frozen, deep-etched, and rotary-replicated Torpedo postsynaptic membrane. J Cell Biol 82:150–173.

Ko C-P. 1984. Regeneration of the active zone at the frog neuromuscular junction. J Cell Biol 98:1685–1695.

Kuffler SW, Nicholls JG, Martin AR. 1984. *From Neuron to Brain: A Cellular Approach to the Function of the Nervous System*, 2nd ed. Sunderland, MA: Sinauer.

McMahan UJ, Kuffler SW. 1971. Visual identification of synaptic boutons on living ganglion cells and of varicosities in postganglionic axons in the heart of the frog. Proc R Soc Lond B Biol Sci 177:485–508.

Miles FA. 1969. *Excitable Cells*. London: Heinemann.

Miyazawa A, Fujiyoshi Y, Unwin N. 2003. Structure and gating mechanism of the acetylcholine receptor pore. Nature 424:949–955.

Morales-Perez CL, Noviello CM, Hibbs RE. 2016. X-ray structure of the human α4β2 nicotinic receptor. Nature 538:411–415.

Noda M, Furutani Y, Takahashi H, et al. 1983. Cloning and sequence analysis of calf cDNA and human genomic DNA encoding α-subunit precursor of muscle acetylcholine receptor. Nature 305:818–823.

Noda M, Takahashi H, Tanabe T, et al. 1983. Structural homology of *Torpedo californica* acetylcholine receptor subunits. Nature 302:528–532.

Palay SL. 1958. The morphology of synapses in the central nervous system. Exp Cell Res 5:275–293. Suppl.

Revah F, Galzi J-L, Giraudat J, Haumont PY, Lederer F, Changeux J-P. 1990. The noncompetitive blocker [3H] chlorpromazine labels three amino acids of the acetylcholine receptor gamma subunit: implications for the alpha-helical organization of regions MII and for the structure of the ion channel. Proc Natl Acad Sci U S A 87:4675–4679.

Salpeter MM (ed). 1987. *The Vertebrate Neuromuscular Junction*, pp. 1–54. New York: Liss.

Takeuchi A. 1977. Junctional transmission. I. Postsynaptic mechanisms. In: ER Kandel (ed). *Handbook of Physiology: A Critical, Comprehensive Presentation of Physiological Knowledge and Concepts*, Sect. 1 *The Nervous System*, Vol. 1 *Cellular Biology of Neurons*, Part 1, pp. 295–327. Bethesda, MD: American Physiological Society.

Verrall S, Hall ZW. 1992. The N-terminal domains of acetylcholine receptor subunits contain recognition signals for the initial steps of receptor assembly. Cell 68:23–31.

Villarroel A, Herlitze S, Koenen M, Sakmann B. 1991. Location of a threonine residue in the alpha-subunit M2 transmembrane segment that determines the ion flow through the acetylcholine receptor-channel. Proc R Soc Lond B Biol Sci 243:69–74.

Walsh J. 1773. Of the electric property of the torpedo. Phil Trans 63(1773):480.

Zeng H, Moise L, Grant MA, Hawrot E. 2001. The solution structure of the complex formed between alpha-bungarotoxin and an 18-mer cognate peptide derived from the alpha 1 subunit of the nicotinic acetylcholine receptor from Torpedo californica. J Biol Chem 276: 22930–22940.

13

Synaptic Integration in the Central Nervous System

Like synaptic transmission at the neuromuscular junction, most rapid signaling between neurons in the central nervous system involves ionotropic receptors in the postsynaptic membrane. Thus, many principles that apply to the synaptic connection between the motor neuron and skeletal muscle fiber at the neuromuscular junction also apply in the central nervous system. Nevertheless, synaptic transmission between central neurons is more complex for several reasons.

First, although most muscle fibers are typically innervated by only one motor neuron, a central nerve cell (such as pyramidal neurons in the neocortex) receives connections from thousands of neurons. Second, muscle fibers receive only excitatory inputs, whereas central neurons receive both excitatory and inhibitory inputs. Third, all synaptic actions on muscle fibers are mediated by one neurotransmitter, acetylcholine (ACh), which activates only one type of receptor (the ionotropic nicotinic ACh receptor). A single central neuron, however, can respond to many different types of inputs, each mediated by a distinct transmitter that activates a specific type of receptor.

These receptors include ionotropic receptors, where binding of transmitter directly opens an ion channel, and metabotropic receptors, where transmitter binding indirectly regulates a channel by activating second messengers. As a result, unlike muscle fibers, central neurons must integrate diverse inputs into a single coordinated action.

Finally, the nerve–muscle synapse is a model of efficiency—every action potential in the motor neuron produces an action potential in the muscle fiber. In comparison, connections made by a presynaptic neuron onto a central neuron are only modestly effective—in many cases at least 50 to 100 excitatory neurons must fire together to produce a synaptic potential large enough to trigger an action potential in postsynaptic neurons.

The first insights into synaptic transmission in the central nervous system came from experiments by John Eccles and his colleagues in the 1950s on the synaptic inputs onto spinal motor neurons that control the stretch reflex, the simple behavior we considered in Chapter 3. The spinal motor neurons have been particularly useful for examining central synaptic mechanisms because they have large, accessible cell bodies and, most important, they receive both excitatory and inhibitory connections and therefore allow us to study the integrative action of the nervous system at the cellular level.

Central Neurons Receive Excitatory and Inhibitory Inputs

To analyze the synapses that mediate the stretch reflex, Eccles activated a large population of axons of the sensory cells that innervate the stretch receptor organs in the quadriceps (extensor) muscle (Figure 13–1A,B). Nowadays the same experiments can be done by stimulating a single sensory neuron.

Passing sufficient current through a microelectrode into the cell body of a stretch-receptor sensory neuron that innervates the extensor muscle generates an action potential. This in turn produces a small excitatory postsynaptic potential (EPSP) in the motor neuron that innervates precisely the same muscle (in this case the quadriceps) monitored by the sensory neuron (Figure 13–1B, upper panel). The EPSP produced by one sensory cell, the unitary EPSP, depolarizes the extensor motor neuron by less than 1 mV, often only 0.2 to 0.4 mV, far below the threshold for generating an action potential. Typically, a depolarization of 10 mV or more is required to reach threshold.

The generation of an action potential in a motor neuron thus requires the near-synchronous firing of a number of sensory neurons. This can be observed in an experiment in which a population of sensory neurons is stimulated by passing current through an extracellular electrode. As the strength of the extracellular stimulus is increased, more sensory afferent fibers are excited, and the depolarization produced by the EPSP becomes larger. The depolarization eventually becomes large enough to bring the membrane potential of the motor neuron axon initial segment (the region with the lowest threshold) to the threshold for an action potential.

In addition to the EPSP produced in the extensor motor neuron, stimulation of extensor stretch-receptor neurons also produces a small inhibitory postsynaptic potential (IPSP) in the motor neuron that innervates the flexor muscle, which is antagonistic to the extensor muscle (Figure 13–1B, lower panel). This hyperpolarizing action is generated by an inhibitory interneuron, which receives excitatory input from the sensory neurons of the extensor muscle and in turn makes synapses with the motor neurons that innervate the flexor muscle. In the laboratory, a single interneuron can be stimulated intracellularly to directly elicit a small unitary IPSP in the motor neuron. Extracellular activation of an entire population of interneurons elicits a larger IPSP. If strong enough, IPSPs can counteract the EPSP and prevent the membrane potential from reaching threshold.

Excitatory and Inhibitory Synapses Have Distinctive Ultrastructures and Target Different Neuronal Regions

As we learned in Chapter 11, the effect of a synaptic potential—whether it is excitatory or inhibitory—is determined not by the type of transmitter released from the presynaptic neuron but by the type of ion channels in the postsynaptic cell activated by the transmitter. Although some transmitters can produce both EPSPs and IPSPs, by acting on distinct classes of ionotropic receptors at different synapses, most transmitters produce a single predominant type of synaptic response; that is, a transmitter is usually inhibitory or excitatory. For example, in the vertebrate central nervous system, neurons that release glutamate typically act on receptors that produce excitation; neurons that release γ-aminobutyric acid (GABA) or glycine act on receptors that produce inhibition.

The synaptic terminals of excitatory and inhibitory neurons can be distinguished by their ultrastructure.

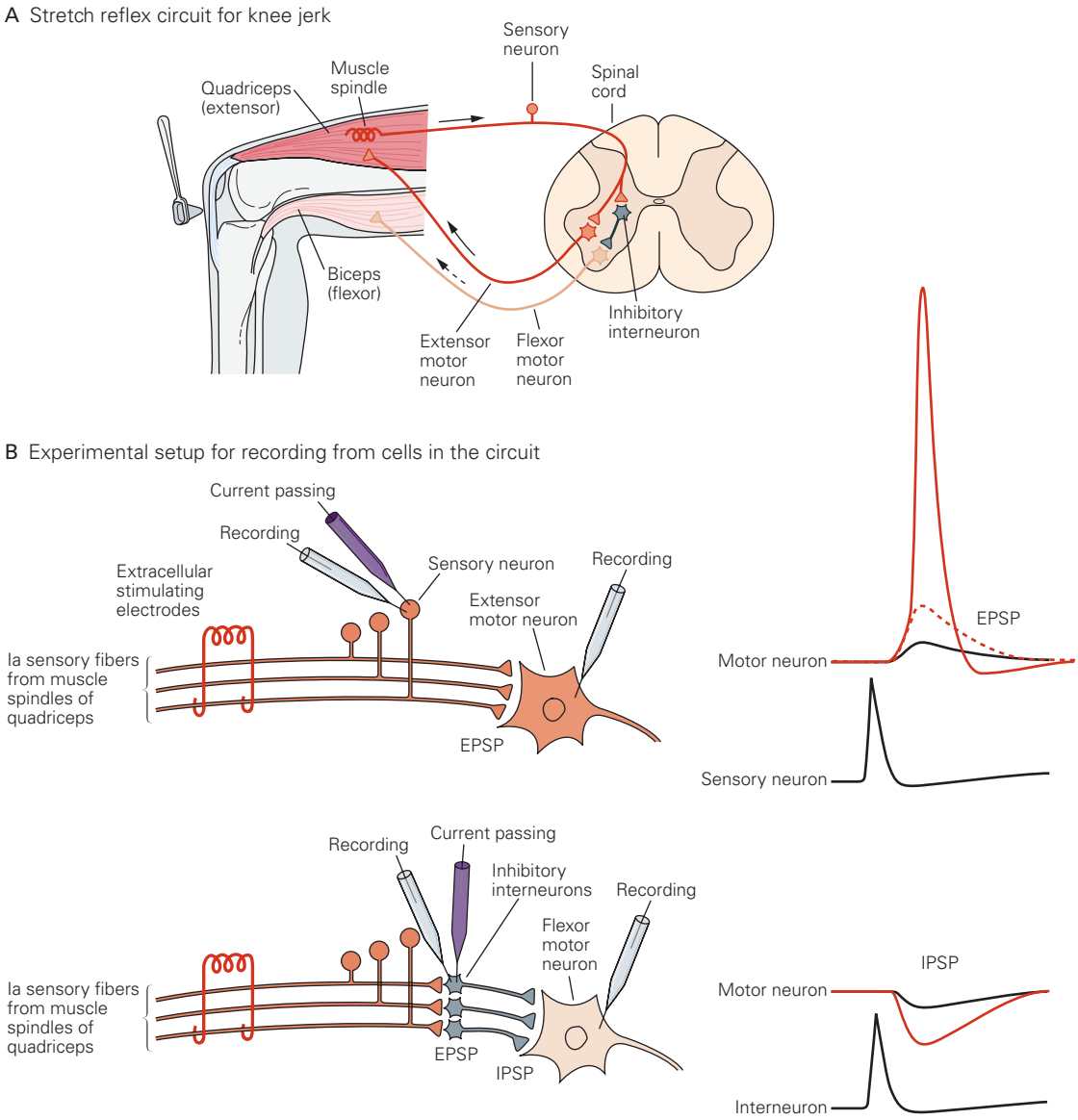

Figure 13–1 **The combination of excitatory and inhibitory synaptic connections mediating the stretch reflex of the quadriceps muscle is typical of circuits in the central nervous system.**

A. A sensory neuron activated by a stretch receptor (muscle spindle) at the extensor (quadriceps) muscle makes an excitatory connection with an extensor motor neuron in the spinal cord that innervates this same muscle group. It also makes an excitatory connection with an interneuron, which in turn makes an inhibitory connection with a flexor motor neuron that innervates the antagonist (biceps femoris) muscle group. Conversely, an afferent fiber from the biceps (not shown) excites an interneuron that makes an inhibitory synapse on the extensor motor neuron.

B. This idealized experimental setup shows the approaches to studying the inhibition and excitation of motor neurons in the pathway illustrated in part A. **Upper panel:** Two alternatives for eliciting excitatory postsynaptic potentials (**EPSPs**) in the extensor motor neuron. A single presynaptic axon can be stimulated by inserting a current-passing electrode into the sensory neuron cell body. An action potential in the sensory neuron stimulated in this way triggers a small EPSP in the extensor motor neuron (**black trace**). Alternatively, the whole afferent nerve from the quadriceps can be stimulated electrically with an extracellular electrode. The excitation of many afferent neurons through the extracellular electrode generates a synaptic potential (**dashed trace**) large enough to initiate an action potential (**red trace**). **Lower panel:** The setup for eliciting and measuring inhibitory potentials in the flexor motor neuron. Intracellular stimulation of a single inhibitory interneuron receiving input from the quadriceps pathway produces a small inhibitory (hyperpolarizing) postsynaptic potential (**IPSP**) in the flexor motor neuron (**black trace**). Extracellular stimulation recruits numerous inhibitory neurons and generates a larger IPSP (**red trace**). (Action potentials in the sensory neuron and interneuron appear smaller because they were recorded at lower amplification than those in the motor neuron.)

Two morphological types of synapses are common in the brain: Gray types I and II (named after E. G. Gray, who described them using electron microscopy). Most type I synapses are glutamatergic and excitatory, whereas most type II synapses are GABAergic and inhibitory. Type I synapses have round synaptic vesicles, an electron-dense region (the *active zone*) on the presynaptic membrane, and an even larger electron-dense region in the postsynaptic membrane opposed to the active zone (known as the *postsynaptic density*), which gives type I synapses an asymmetric appearance. Type II synapses have oval or flattened synaptic vesicles and less obvious presynaptic membrane specializations and postsynaptic densities, resulting in a more symmetric appearance (Figure 13–2). (Although type I synapses are mostly excitatory and type II inhibitory, the two morphological types have proved to be only a first approximation to transmitter biochemistry. Immunocytochemistry affords much more reliable distinctions between transmitter types, as discussed in Chapter 16).

Although dendrites are normally postsynaptic and axon terminals presynaptic, all four regions of the nerve cell—axon, presynaptic terminals, cell body, and dendrites—can be presynaptic or postsynaptic sites of chemical synapses. The most common types of contact, illustrated in Figure 13–2, are axodendritic, axosomatic, and axo-axonic (by convention, the presynaptic element is identified first). Excitatory synapses are typically axodendritic and occur mostly on dendritic spines. Inhibitory synapses are normally formed on dendritic shafts, the cell body, and the axon initial segment. Dendrodendritic and somasomatic synapses are also found, but they are rare.

As a general rule, the proximity of a synapse to the axon initial segment is thought to determine its effectiveness. A given postsynaptic current generated at a site near the cell body will produce a greater change in membrane potential at the trigger zone of the axon initial segment, and therefore have a greater influence on action potential output than an equal current generated at more remote sites in the dendrites. This is because some of the charge entering the postsynaptic membrane at a remote site will leak out of the dendritic membrane as the synaptic potential propagates to the cell body (Chapter 9). Some neurons compensate for this effect by placing

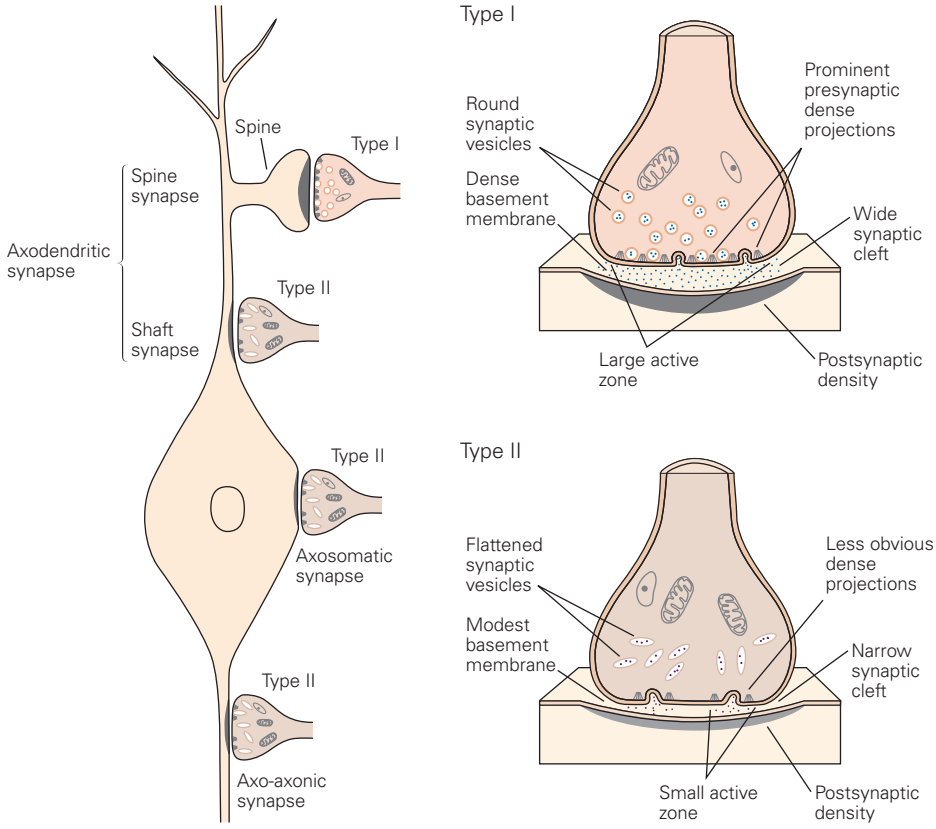

Figure 13–2 The two most common morphological types of synapses in the central nervous system are Gray type I and type II. Type I is usually excitatory, whereas type II is usually inhibitory. Differences include the shape of vesicles, the prominence of presynaptic densities, total area of the active zone, width of the synaptic cleft, and presence of a dense basement membrane. Type I synapses typically contact specialized dendritic projections, called spines, and less commonly contact the shafts of dendrites. Type II synapses contact the cell body (axosomatic), dendritic shaft (axodendritic), axon initial segment (axo-axonic), and presynaptic terminals of another neuron (not shown).